

# BRAHMS Overview

**Ramiro Debbe† for the BRAHMS Collaboration**

† Brookhaven National Laboratory, Upton NY, 11973

**Abstract.** A brief review of BRAHMS measurements of bulk particle production in RHIC’s Au+Au collisions at  $\sqrt{s_{NN}} = 200\text{GeV}$  is presented, together with some discussion of baryon number transport. Intermediate  $p_T$  measurements in different collision systems (Au+Au, d+Au and p+p) are also discussed in the context of jet quenching and saturation of the gluon density in Au ions at RHIC energies. This report also includes preliminary results for identified particles at forward rapidities.

## 1. Introduction

The bulk of particle production in high energy hadron collisions continues to be a not fully understood phenomenon. Even though these collisions can be modeled with varying degrees of accuracy, a solution from “first principles” is still being sought. The BRAHMS collaboration at RHIC has set out to measure the bulk particle production in as wide as possible range in rapidity and with good particle identification and momentum resolution. That wide rapidity range offers an almost complete coverage that allows for the inclusion of conservation laws whenever a description of the physics behind the collisions is proposed. This contribution starts with a brief summary of some of the most relevant measurements of bulk particle production.

The production of jets at RHIC energies is well established and, one of the most dramatic discoveries in Au+Au collisions at full energy has been the suppression of those jets as they traverse a highly opaque medium formed by the collisions [1] and [2]. BRAHMS can also study jet production through the measurement of leading particles up to intermediate values of transverse momentum ( $\sim 4\text{GeV}/c$ ). Our ability to identify the particles we measure, together with our reach to high values of rapidity, make BRAHMS intermediate  $p_T$  measurements very relevant in the study of the new medium formed in Au+Au collisions along the longitudinal component of momentum, or more precisely as function of rapidity. The high rapidity reach has also been instrumental in the study of charged particle production in d+Au collisions compared to incoherently added p+p collisions. The evolution of this comparison with rapidity and the centrality of the collision will be review in this presentation. Finally preliminary results from the analysis of Au+Au and d+Au collisions are presented in the last section. More details about BRAHMS results can be found in our “white paper” [3].

## 2. Experimental setup

The BRAHMS setup consists of two rotatable spectrometers, the mid-rapidity spectrometer (MRS) and the forward spectrometer (FS), complemented with an event characterization system used to determine the geometry of the collisions. The MRS spectrometer measures the momentum of charged with two tracking stations (time projection chambers) and a single dipole magnet. Particle identification in this spectrometer is done with time-of-flight hodoscopes and a

threshold Cherenkov detector. Details about the performance of the MRS spectrometer can be found in Ref. [?]. The FS spectrometer measures the much higher momenta of charged particles produced at small angles with five tracking stations (two TPC and three drift chambers). Particle identification in the FS spectrometer is done with a complement of two time-of-flight hodoscopes, one threshold Cherenkov counter and a Ring Imaging Cherenkov detector. A detailed description of the BRAHMS experimental setup can be found in [6]. The geometry of the collisions is extracted from the multiplicity of charged particles measured in the  $|\eta| \leq 2.2$  range [7]. The normalization of our measurements is obtained with minimum biased triggers designed to maximize the coverage of the inelastic cross section. In Au+Au collisions that trigger was defined with the Zero Degrees calorimeters ZDC and for the p+p and d+Au collisions we used a set of scintillators around the beam pipe.

### 3. Rapidity densities

The rapidity densities for the most central data sample ( $0 - 5\%$ ) in Au+Au collisions at  $\sqrt{s_{NN}} = 200\text{GeV}$  have been obtained by integration of the invariant differential yields  $\frac{1}{2\pi} \frac{d^2N}{p_T dp_T dy}$  at several intervals of rapidity. The measurement of very low values of transverse momentum  $p_T$  is limited by multiple scattering and particle decay, an interpolation is thus necessary in order to integrate the yields all the way down to zero  $p_T$ . Power law functions were used to integrate the pion distributions and single exponentials in  $m_T - m_0$  for the kaon distributions [4]. Protons were fitted with single gaussians [5]. The result of these integrals is shown in Fig. 1. The shape of the produced particles densities (pions, kaons and anti-protons) is remarkably Gaussian. The width of the negative pion distribution is equal to:  $\sigma_{\pi^-} = 2.29 \pm 0.02$ . The widths of the rapidity densities of pions, kaons and anti-protons are very similar, and at the same time different from the ones associated with a single thermal source. A hydrodynamical description of the system is considered as the best approach to explain this wide distributions, even though hydrodynamical models [9], have not yet been able to reproduce the rapidity dependence of the so called elliptic flow [8].

Panel c of Fig. 1 shows the measured rapidity density for protons and anti-protons and panel d shows the net-proton density as function of rapidity after corrections from hyperon feed down. From this measurement an average rapidity loss of 2 units of rapidity has been deducted. The fact that the net proton around mid-rapidity is considerably different from zero suggests that there are other mechanisms besides valence quark transport to move baryon number to mid-rapidity. Baryon junctions are considered as good candidates because their small-x component would be a natural way to place finite baryon number at  $y \sim 0$  [10]. More details of this measurement can be found in ref. [5].

With the measurements described above, there is enough information to do an energy balance of the Au+Au collisions at  $\sqrt{s_{NN}} = 200\text{GeV}$ . With reasonable assumptions about the particles that were not measured, and allowing for some 10 – 15% error in the extrapolation up to beam rapidity, we find that 25 TeV out of the 33 TeV of total energy is found in produced particles. The energy of the extrapolated net baryon distribution has been found to be  $27 \pm 6\text{GeV}$  (see Ref. [5]), leaving  $73 \pm 6\text{GeV}$ , out of the 100 GeV of each incoming nucleon, available for particle production, well in agreement with the result obtained from the energy balance per particle species.

### 4. Intermediate $p_T$ studies and the nuclear modification factors

As mentioned in the introduction, the study of intermediate  $p_T$  distributions produced one of the most important results from RHIC; compared to appropriately scaled p+p collisions, it was found that the yields in Au+Au collisions were reduced by almost a factor of five [1] and [2]. Such reduction in yield was soon identified as energy loss in a dense and opaque medium. The particles detected being the leading particles of jets formed by partons traversing the medium

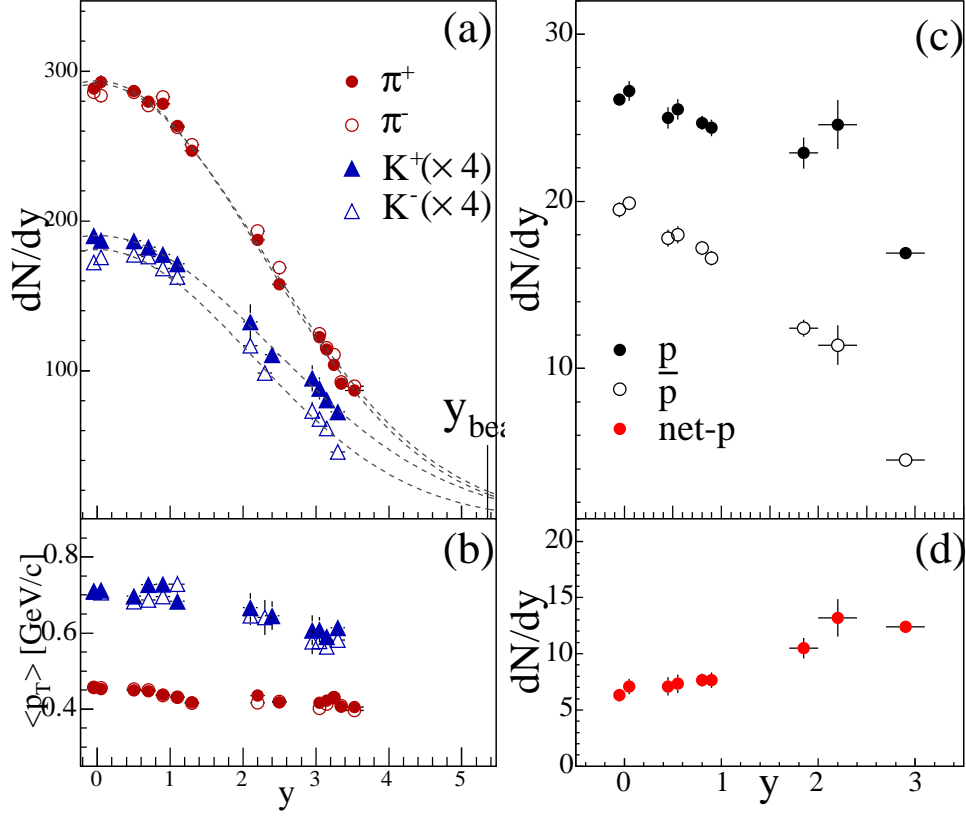


**Figure 1.** (a) Rapidity densities for pions and kaons. (b) Mean transverse momentum for pions, kaons and protons. (c) Rapidity density of protons and anti-protons. (d) Net proton rapidity densities corrected for hyperon feed-down.

while their energy is degraded by multiple interactions where the main process would be gluon bremsstrahlung. Similar measurements performed in d+Au collisions at the same energy did not show the same strong suppression at mid-rapidity but rather an enhancement [11] that is understood as multiple elastic scatterings at the partonic level before the interaction that produced the jet whose leading particle is detected. The dominant source of the suppression measured in Au+Au collisions would then be the final state interaction of the partons with an opaque medium. BRAHMS extended a similar study to higher values of rapidity and found that the description of the enhancement measured at mid-rapidity was not applicable at forward rapidities where in fact we found again a suppression [12].

Figure 2 shows the nuclear modification factor defined as  $R_{dAu} = \frac{1}{N_{coll}} \frac{\frac{dN^{dAu}}{dp_T d\eta}}{\frac{dN^{pp}}{dp_T d\eta}}$ , where  $N_{coll}$  is the number of binary collisions estimated to be equal to  $7.2 \pm 0.6$  for minimum biased d+Au collisions. Each panel shows the ratio calculated at a different  $\eta$  value. At mid-rapidity ( $\eta = 0$ ), the nuclear modification factor exceeds 1 for transverse momenta with values greater than 2 GeV/c in similar, although less pronounced, way as Cronin's p+A measurements performed at lower energies [15].

A shift of one unit of rapidity is enough to make the Cronin type enhancement disappear, and as the measurements are done at higher rapidities, the ratio becomes consistently smaller than 1 indicating a suppression in d+Au collisions compared to scaled p+p systems at the same

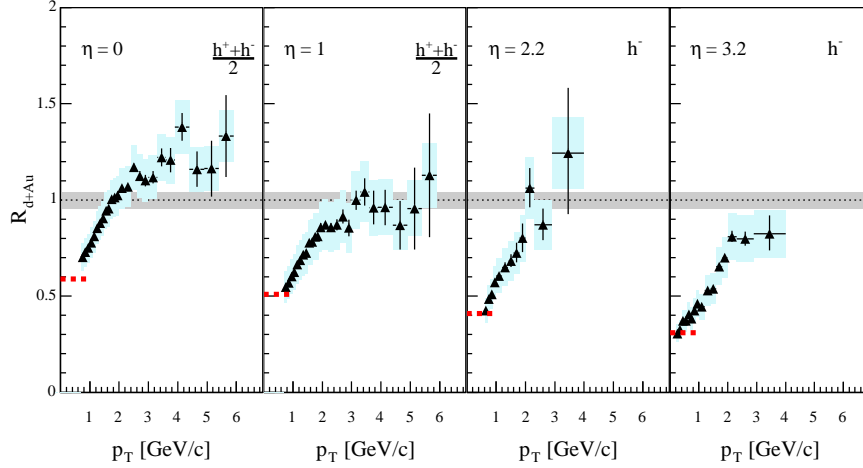


**Figure 2.** Nuclear modification factor for charged hadrons at pseudorapidities  $\eta = 0, 1.0, 2.2, 3.2$ . Statistical errors are shown with error bars. Systematic errors are shown with shaded boxes with widths set by the bin sizes. The shaded band around unity indicates the estimated error on the normalization to  $\langle N_{coll} \rangle$ . Dashed lines at  $p_T < 1$  GeV/c show the normalized charged particle density ratio  $\frac{1}{\langle N_{coll} \rangle} \frac{dN/d\eta(d+Au)}{dN/d\eta(pp)}$ .

energy.

In all four panels, the statistical errors, shown as error bars (vertical lines), are dominant specially in our most forward measurements. Systematic errors are shown as shaded rectangles. An additional systematic error is introduced in the calculation of the number of collisions  $N_{coll}$  that scales the d+Au yields to a nucleon-nucleon system. That error is shown as a 15% band at  $R_{dAu} = 1$ .

The evolution as function of rapidity seen in Fig. 2 is more obvious for samples of central events. The four panels of Fig. 3 show the central  $R_{CP}^{central}$  (filled symbols) and semi-central  $R_{CP}^{semi-central}$  (open symbols) ratios for the for  $\eta$  settings. Starting on the left panel corresponding to  $\eta = 0$ , the central events yields are systematically higher than those of the semi-central events, but at the highest pseudo-rapidity  $\eta = 3$ , the yields of central events are  $\sim 60\%$  lower than the semi-central events for all values of transverse momenta.

These results have generated much interest in the community because they appear as another indication of the onset of the so called Color Glass Condensate [13] at RHIC energies and high atomic numbers ( $A=179$  for the gold ions) [16].

The analysis of the BRAHMS data from d+Au and p+p collisions is currently in progress, in particular, Fig. 4 presents the nuclear modification  $R_{dAu}$  for anti-protons and negative pions at  $\eta = 3.2$ . This ratios were obtained making the following assumption: point by point one can extract the ratios for identified particles by multiplying the numerator and the denominator by the fraction of identified particles with respect to the negative charged particles:

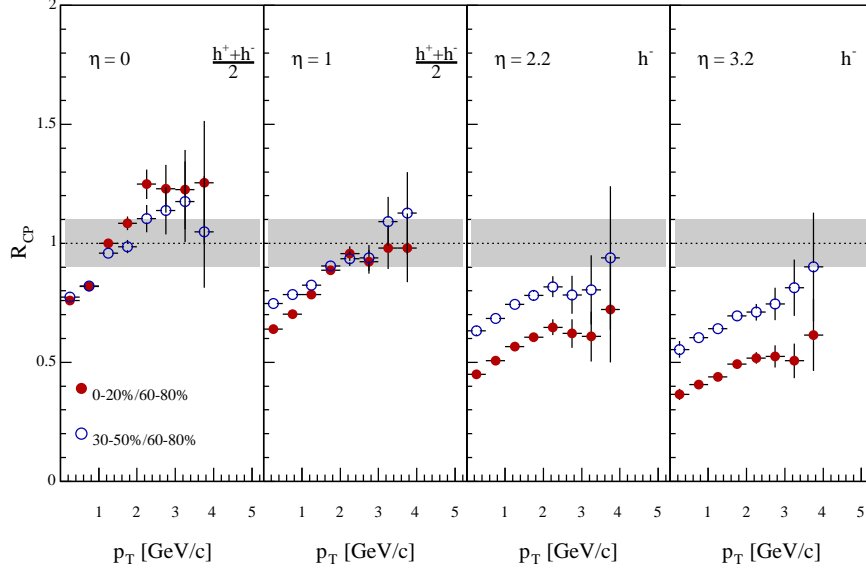


**Figure 3.** Central (full points) and semi-central (open points)  $R_{cp}$  ratios (see text for details) at pseudorapidities  $\eta = 0, 1.0, 2.2, 3.2$ . Systematic errors ( $\sim 5\%$ ) are smaller than the symbols. The ratios at the highest pseudorapidities ( $\eta = 2.2$  and  $3.2$ ) are calculated for negative hadrons. The uncertainty on the normalization of the ratios is displayed as a shaded band around unity. Its value has been set equal to the error in the calculation of  $N_{coll}$  in the most peripheral collisions (12%).

$$R_{dAu}^{\bar{p}} = R_{dAu}^{h^-} \frac{\left(\frac{\bar{p}}{h^-}\right) dAu}{\left(\frac{\bar{p}}{h^-}\right) pp} = \frac{1}{N_{coll}} \frac{\left(\frac{dn^{dAu}}{dp_T d\eta}\right)^{h^-}}{\left(\frac{dn^{pp}}{dp_T d\eta}\right)^{h^-}} \frac{\left(\frac{dn^{dAu}}{dp_T d\eta}\right)^{\bar{p}}}{\left(\frac{dn^{pp}}{dp_T d\eta}\right)^{\bar{p}}} = \frac{1}{N_{coll}} \frac{\left(\frac{dn^{dAu}}{dp_T d\eta}\right)^{\bar{p}}}{\left(\frac{dn^{pp}}{dp_T d\eta}\right)^{\bar{p}}}$$

The ratio of raw counts is then equated with the ratio of differential yields in  $\eta$  and  $p_T$ , assuming that all corrections do cancel out. The ratio of raw counts was obtained with information from the Ring Imaging Cherenkov detector whose efficiency is high ( $\sim 95\%$ ) but has not been included in this analysis. The errors shown for the nuclear modification factors of anti-protons and pions include the contributions from correlations between the parameters of the fit made to the raw ratios. No attempt was made to estimate the contributions to the anti-proton result from feed down from anti-lambdas. The remarkable difference between baryons and mesons has also been seen at RHIC energies around mid-rapidity.

At the time the invariant yields at  $\eta = 3.2$  were shown for the first time, the clear difference between positive and negative charged particles prompted some to associate the suppression seen in d+Au collisions at forward angles with the so called “beam fragmentation” [18]. More recent works based on NLO pQCD have indicated the difficulty in reconciling the data with the behavior of standard fragmentation functions [19]. Panel a of Fig. 5 shows that, as expected, there are as many protons as positive pions ( $\sim 80\%$ ) in the positive charged particle distribution

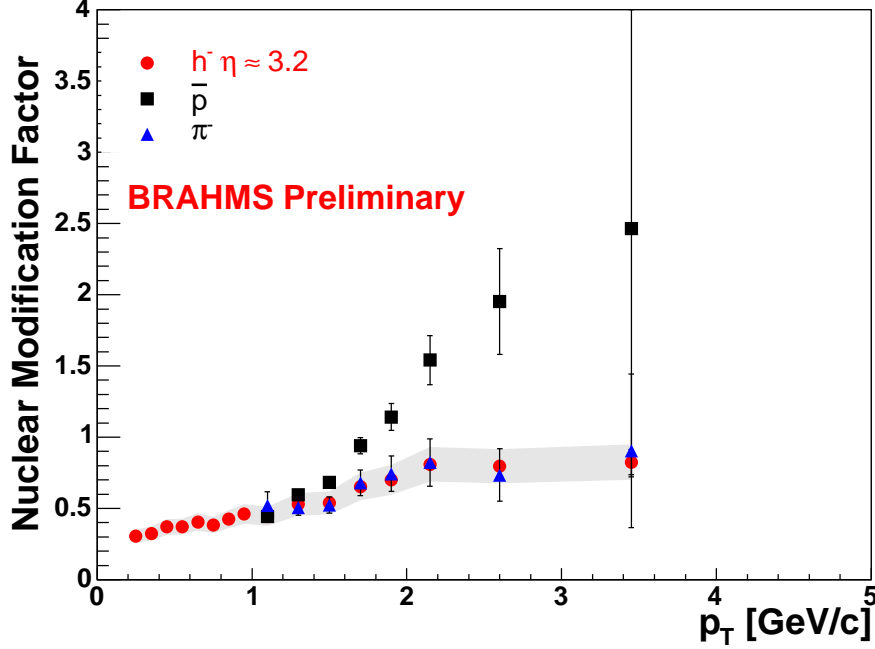


**Figure 4.** The nuclear modification factor  $R_{dAu}$  calculated for anti-protons (filled squares) and negative pions (filled triangles) at  $\eta = 3.2$ . The same ratio calculated for negative particles at the same pseudo-rapidity [12] is shown with filled circles, and the systematic error for that measurement is shown as grey band.

at  $\eta = 3.2$ . Panel b of the same figure shows that for all values of  $p_T$ , the fraction of negative pions is high and equal to 80%.

The comparison of particle production at mid-rapidity in Au+Au central collisions to that from incoherently added p+p interactions, or properly scaled distributions obtained from peripheral Au+Au collisions is widely accepted as a necessary condition for a momentum degradation related to gluon radiation as partons traverse an opaque medium before hadronization. That degradation is expected to depend on the length of the path as well as the density of the medium [17]. Such partonic energy loss is encoded in a medium modified fragmentation function that fragments in the standard way but only after the energy has been degraded by several interactions in the medium distributed in number according to a Poisson distribution with a mean value equal to  $L/\sigma\rho$  where  $L$  is the parton path length in the medium and  $\sigma$  is the interaction cross-section and  $\rho$  the medium density. The final fragmentation also includes the gluons radiation at each interaction. The pion rapidity density should be directly related to the medium density and as can be seen in Fig. 1 between mid-rapidity and  $y = 3$ , there is a reduction in the rapidity density by almost a factor of three. One would then expect less energy loss at  $y=3$ , by a comparable factor, but as can be seen in Fig. 6, there is no noticeable change in the amount of  $p_T$  suppressions as the measurements are done at higher rapidities. Moreover, the value of  $R_{CP}$  does not change between  $y=0$  and 3!

In summary, BRAHMS has studied the properties of bulk particle production as well as baryon number transport in Au+Au collisions at  $\sqrt{s_{NN}} = 200 \text{ GeV}/c$ . We have also compared charged particle production in Au+Au and d+Au collisions to similar production in p+p collisions at the same energy. Such comparisons show strong suppression at intermediate

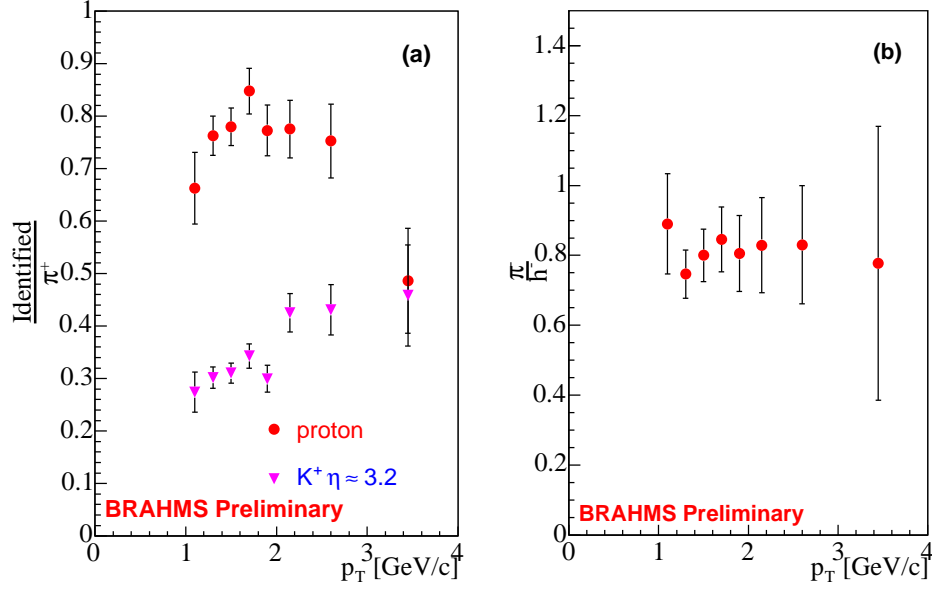


**Figure 5.** Some results with pid at  $\eta = 3.2$ : (a) Particle composition of positive charged hadrons at  $\eta = 3.2$  (b) The fraction of negative hadrons identified as pions at the same pseudo-rapidity.

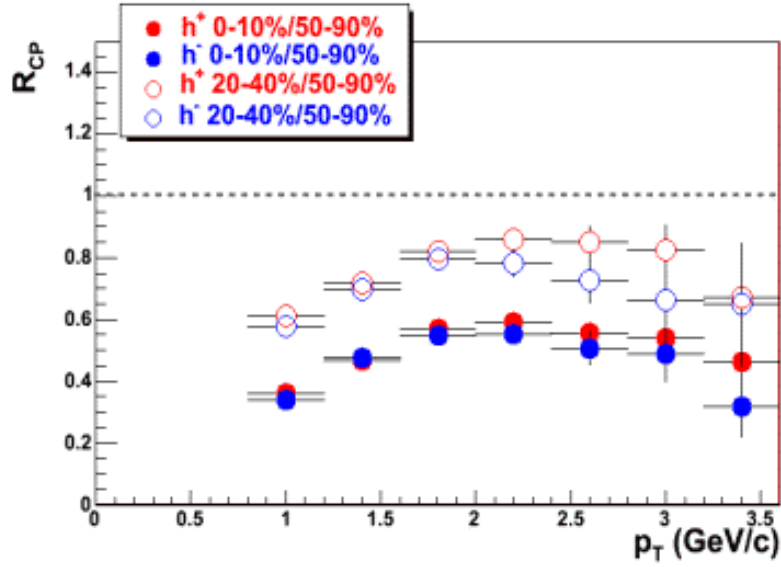


**Figure 6.** Preliminary  $R_{CP}$  of charged particles from Au+Au at  $\eta = 3.2$

transverse momentum associated with the formation of a dense and opaque medium. Such suppression doesn't appear at mid-rapidity in d+Au collisions but it is present at forward rapidities and is even more pronounced for central collisions.

## 5. Acknowledgments

This work was supported by the Office of Nuclear Physics of the U.S. Department of Energy, the Danish Natural Science Research Council, the Research Council of Norway, the Polish State Committee for Scientific Research (KBN) and the Romanian Ministry of Research.

## References

- [1] K. Adcox *et al.*, PHENIX Collaboration, Phys. Rev. Lett. **88** 022301 (2002); S. S. Adler *et al.*, STAR Collaboration, Phys. Rev. Lett. **89** 202301 (2002); B.B. Back, *et al.*, PHOBOS Collaboration, Phys. Lett. B **578**, 297 (2004).
- [2] I. Arsene *et al.*, BRAHMS Collaboration, Phys. Rev. Lett. **91**, 072305 (2003).
- [3] I. Arsene *et al.*, BRAHMS Collaboration, Submitted to Nuc. Phys A nucl-ex/0410020 (2004).
- [4] I.G. Bearden *et al.*, Submitted to Phys. Rev. Lett. (nucl-ex/0403050).
- [5] I. G. Bearden *et al.* Phys. Rev. Lett. **93**, 102301 (2004).
- [6] M. Adamczyk *et al.*, BRAHMS Collaboration, Nuclear Instruments and Methods A **499** 437 (2003).
- [7] Y.K. Lee *et al.*, Nuclear Instruments and Methods A **499** 437 (2003).
- [8] B.B. Back, *et al.*, PHOBOS Collaboration, Phys. Rev. C (Rapid Comm.) (2004).
- [9] T. Hirano and Y. Nara, Nucl. Phys. A **743**, 305 (2004).
- [10] D. Kharzeev Phys. Lett. B **378**, 238-246, (1996).
- [11] B.B. Back *et al.*, PHOBOS Collaboration, Phys. Rev. Lett. **91**, 72302 (2003); S.S. Adler *et al.*, STAR Collaboration, Phys. Rev. Lett. **91**, 72303 (2003); J. Adams *et al.*, PHENIX Collaboration, Phys. Rev. Lett. **91**, 72304 (2003).
- [12] I. Arsene *et al.*, Phys. Rev. Lett. **93**, 242303 (2004).
- [13] L. McLerran and R. Venugopalan, Phys. Rev. D **49**, 2233 (1994), Phys. Rev. D **49**, 3352 (1994), Phys. Rev. D **50**, 2225 (1994), Phys. Rev. D **59**, 094002 (1999); Y. V. Kovchegov, Phys. Rev. D **54**, 5463 (1996), Phys. Rev. D **55**, 5445 (1997).
- [14] I. Arsene *et al.*, Submitted to Phys. Rev. Lett. (nucl-ex/0401025).
- [15] D. Antreasyan *et al.*, Phys. Rev. D **19**, 764 (1979).
- [16] D. Kharzeev, Y. V. Kovchegov and K. Tuchin Phys. Rev. D **68**, 094013, (2003), hep-ph/0307037; D. Kharzeev, E. Levin and L. McLerran, Phys. Lett. B **561**, 93 (2003); R. Baier, A. Kovner and U. A. Wiedemann Phys. Rev. D **68**, 054009, (2003); J. Albacete, *et al.* hep-ph/0307179.; A. Dumitru and J. Jalilian-Marian, Phys. Lett. B **547**, 15 (2002); J. Jalilian-Marian, A. Kovner, A. Leonidov, H. Weigert, Phys. Rev. D **59**, 014014 (1999). J. Jalilian-Marian *et al.* Phys. Lett. B **577**, 54-60 (2003), nucl-th/0307022;
- [17] X. N. Wang and Z. Huang, Phys. Rev. C **55**, 3047, (1997).
- [18] M. Gyulassy Proceedings RIKEN Workshop Volume **57**, 141 Dec. 2-6 (2003).
- [19] V. Guzey, M. Strickman, W. Vogelsang, Phys. Lett. D **603**, 173 (2004).